Northward dispersal of dinosaurs from Gondwana to Greenland at the mid-Norian (215–212 Ma, Late Triassic) dip in atmospheric pCO_2

Dennis V. Kent[a,b,1] and Lars B. Clemmensen[c]

[a]Paleomagnetics Lab, Lamont-Doherty Earth Observatory of Columbia University, Palisades, NY 10964; [b]Department of Earth and Planetary Sciences, Rutgers University, Piscataway, NJ 08854; and [c]Department of Geosciences and Natural Resource Management, University of Copenhagen, DK-1350 Copenhagen, Denmark

Edited by Lisa Tauxe, University of California San Diego, La Jolla, CA, and approved January 7, 2021 (received for review October 4, 2020)

The earliest dinosaurs (theropods and sauropodomorphs) are found in fossiliferous early Late Triassic strata dated to about 230 million years ago (Ma), mainly in northwestern Argentina and southern Brazil in the Southern Hemisphere temperate belt of what was Gondwana in Pangea. Sauropodomorphs, which are not known for the entire Triassic in then tropical North America, eventually appear 15 million years later in the Northern Hemisphere temperate belt of Laurasia. The Pangea supercontinent was traversable in principle by terrestrial vertebrates, so the main barrier to be surmounted for dispersal between hemispheres was likely to be climatic; in particular, the intense aridity of tropical desert belts and unstable climate in the equatorial humid belt accompanying high atmospheric pCO_2 that characterized the Late Triassic. We revisited the chronostratigraphy of the dinosaur-bearing Fleming Fjord Group of central East Greenland and, with additional data, produced a correlation of a detailed magnetostratigraphy from more than 325 m of composite section from two field areas to the age-calibrated astrochronostratigraphic polarity time scale. This age model places the earliest occurrence of sauropodomorphs (*Plateosaurus*) in their northernmost range to ∼214 Ma. The timing is within the 215 to 212 Ma (mid-Norian) window of a major, robust dip in atmospheric pCO_2 of uncertain origin but which may have resulted in sufficiently lowered climate barriers that facilitated the initial major dispersal of the herbivorous sauropodomorphs to the temperate belt of the Northern Hemisphere. Indications are that carnivorous theropods may have had dispersals that were less subject to the same climate constraints.

magnetostratigraphy | Triassic | dinosaurs | Pangea | paleoclimate

Some of the earliest documented occurrences of true dinosaurs are in the Ischigualasto Formation of northwestern Argentina (1, 2) and the Santa Maria Formation of southern Brazil (3) that were part of Gondwana and are of late Carnian age as indicated by high precision U-Pb zircon dates of 229 to 233 Ma (4, 5). These early Late Triassic dinosaurs occur at paleolatitudes of about 50°S (6). Gondwana and the northern continent assembly of Laurasia constituted most of the world landmasses in the supercontinent of Pangea, whose contiguous extent should have posed no obvious physical barriers to latitudinal dispersal of land vertebrates. Nonetheless, the earliest documented dinosaur occurrences in Laurasia (7) are typically attributed to the succeeding Norian Stage, as in the Chinle Formation of the North American Southwest, the Keuper Group in Germany, and the Fleming Fjord Group of central East Greenland, which is the northernmost occurrence of dinosaurs in the Late Triassic at ∼43°N (8) (Fig. 1).

The chronostratigraphy of the Chinle Formation has been significantly improved recently with integrated results from the Colorado Plateau Coring Project (9–11). These data strongly validate the Newark-Hartford astrochronostratigraphic polarity time scale [APTS; (12)] for synchronizing Late Triassic stratigraphic sequences and their fossil assemblages around the globe. Here, we present an updated chronology for the Fleming Fjord Group of Greenland based on a magnetostratigraphy (13) expanded by data from a second sampling area, which necessitates a revised older-age assignment for the documented fossil occurrences of plateosaurid *Plateosaurus* (14–16). Together, with an assessment linked to the APTS of the age of the Löwenstein Formation in the Germanic basin that has the earliest occurrences of *Plateosaurus* in Europe (17), we are able to chart a more precise temporal pattern of the dispersal of early sauropodomorph dinosaurs that can be compared to well-dated records of atmospheric partial pressure of carbon dioxide (pCO_2) concentrations to explore climate change as a contributing factor.

Results

Magnetostratigraphy of Fleming Fjord Group Sections. The Fleming Fjord Group [elevated in rank from Formation (18)] is composed of fluvial and lacustrine sediments about 350 m thick, subdivided in upward succession into the Edderfugledal, Malmros Klint, and Ørsted Dal formations [elevated in rank from members (18)]. The Fleming Fjord Group overlies, in apparent conformity, the Gipsdalen Group, but the overlying Kap Stewart Group, which records the end-Triassic event (ETE) (19), is likely to be disconformable with an intervening break in sedimentation (20).

Paleomagnetic sampling of outcrop sections at Tait Bjerg (Fig. 2) was included in the summer 1992 field season to help constrain the age of the rich vertebrate fauna (14). A magnetostratigraphy with seven magnetozones from F1n at the base up to F4n were delineated

Significance

Sharply contrasting climate zonations under high atmospheric pCO_2 conditions can exert significant obstacles to the dispersal of land vertebrates across a supercontinent. This is argued to be the case in the Triassic for herbivorous sauropodomorph dinosaurs, which were confined to their initial venue in the Southern Hemisphere temperate belt of Pangea for about their first 15 million years. Sauropodomorphs only appear in the fossil record of the Northern Hemisphere temperate belt about 214 million years ago based on a composite magnetostratigraphy of the Fleming Fjord Group in East Greenland. The coincidence in timing within a major dip in atmospheric pCO_2 from published paleosol records suggests the dispersal was related to a concomitant attenuation of climate barriers in a greenhouse world.

Author contributions: D.V.K. designed research; D.V.K. and L.B.C. performed research; D.V.K. and L.B.C. analyzed data; and D.V.K. wrote the paper.

The authors declare no competing interest.

This article is a PNAS Direct Submission.

[1]To whom correspondence may be addressed. Email: dvk@ldeo.columbia.edu.

This article contains supporting information online at https://www.pnas.org/lookup/suppl/doi:10.1073/pnas.2020778118/-/DCSupplemental.

Published February 15, 2021.

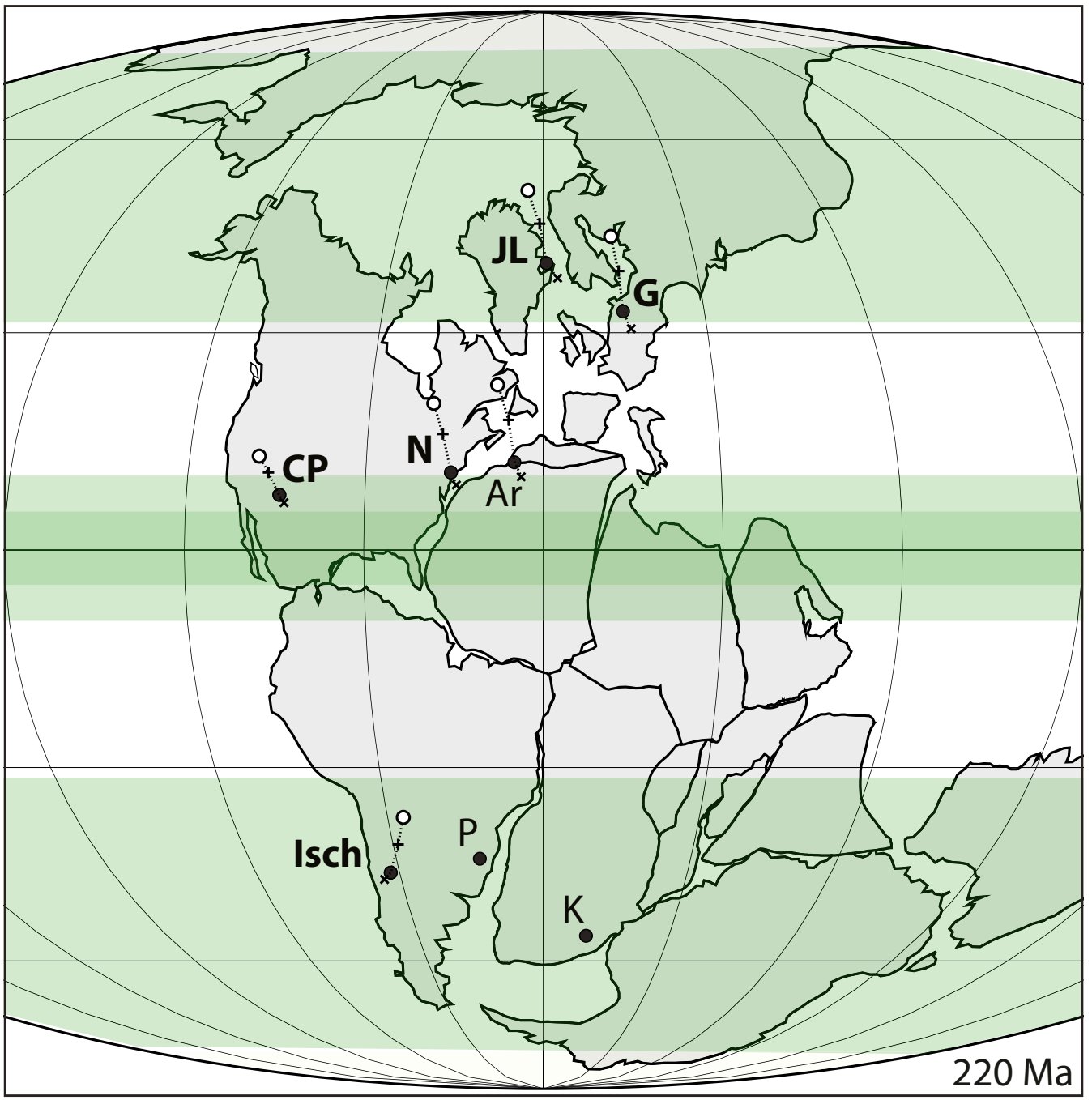

Fig. 1. The locations of Jameson Land (JL) and some other Late Triassic vertebrate fossil localities discussed in text are labeled as follows: Ar, Argana basin; CP, Colorado Plateau (Chinle Formation); G, Germanic basin (Keuper Group, Löwenstein Formation); Isch, Ischigualasto-Villa Union basin; K, Karoo basin (lower Elliot Formation); N, Newark basin; and P, Parana basin (Santa Maria Formation) shown as solid circles on a reconstruction of Pangea for the Norian Stage, positioned using the 220-Ma mean global pole from ref. 36 and showing the relative position of key sites at 230 Ma as x's, 210 Ma as crosses, and 200 Ma by open circles as Pangea drifted northward. The idealized zonal belts (62) of precipitation relative to evaporation are indicated by green shading for P > E (more humid) and grading to open shading for P < E (more arid).

in a ~210-m outcrop section of the Malmros Klint and the lower part of the Ørsted Dal formations (13) (Fig. 3). Paleomagnetic samples were also collected during the summer 1995 field season of fossil hunting at "Track Mountain" near MacKnight Bjerg (Fig. 2) from a ~100-m-thick section of the Carlsberg Fjord and Tait Bjerg members of the Ørsted Dal Formation and about a 40-m section of the upper Edderfugledal and lowermost Malmros Klint formations. The samples were processed in the same manner as described for the summer 1992 field season samples, featuring comprehensive progressive thermal demagnetization to isolate a characteristic magnetization from a pervasive Cenozoic overprint (*SI Appendix*). The "Track Mountain" data were thus far only used (in conjunction with the Tait Bjerg results) for a statistical analysis of Late Triassic paleolatitudes (8). Based on the overall lithostratigraphy, the newly realized polarity magnetozones in the "Track Mountain" section extend from the top of F2r in the lower Carlsberg Fjord Member to F5n in the upper part of the Tait Bjerg Member, whereas magnetozones F0r and F1n could be

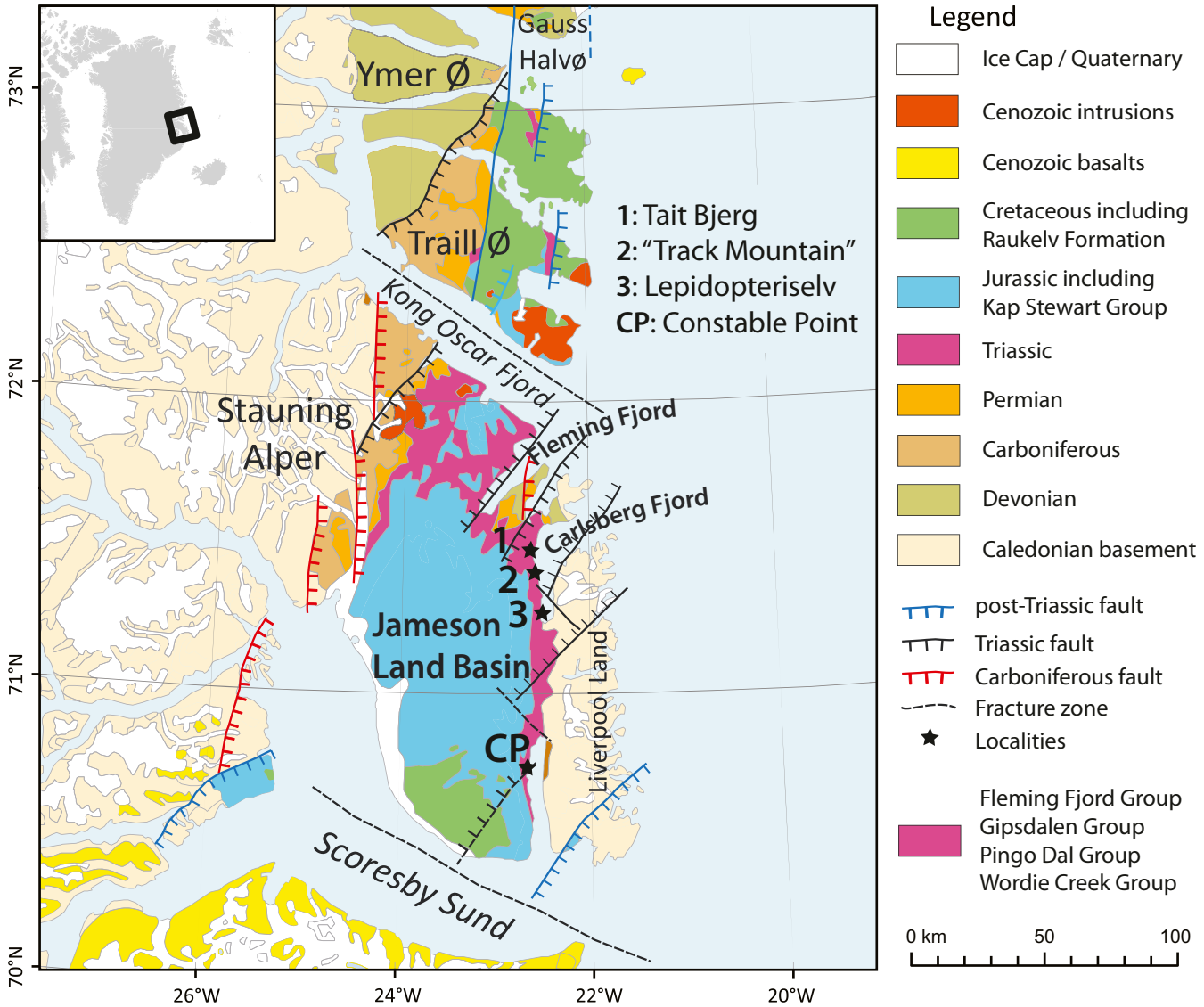

Fig. 2. Paleomagnetic sampling and other relevant localities in Jameson Land, central East Greenland, including the following: 1: Tait Bjerg, 1992 field season; 2: "Track Mountain" near MacKnight Bjerg, 1995 field season; 3: Lepidopteriselv; and CP: Constable Point. The map is adapted from ref. 18, which is licensed under CC BY 4.0, and published with the permission of the Geological Society of Denmark.

identified in the Edderflugledal and lowermost Malmros Klint formations in the "Stairmaster" section located 15 km northwest of the Tait Bjerg section (Fig. 3 and *SI Appendix*, Tables S1 and S2).

The base of magnetozone F3n in the lower part of the Carlsberg Fjord Member of the Ørsted Dal Formation at 213 m from the base of the Edderfugledal Formation in the Tait Bjerg section and at 6.5 m above the local base of the Carlsberg Fjord Member in the MacKnight Bjerg section serves as a tiepoint for assembling a composite magnetostratigraphy some 325 m thick (*SI Appendix*, Table S3). The match of magnetozones between the overlapping portions of the sections is unequivocal, giving us confidence that the polarity sequence is correctly delineated and allowing us to extend the magnetostratigraphy upward from the upper Carlsberg Fjord Member into the Tait Bjerg Member of the Ørsted Dal Formation as well as downward from the lowermost Malmros Klint into the Edderfulgedal formations (Fig. 3). A total of 12 magnetozones are identified, although 3 (F0r, F4r, and F5n) more tentatively by only single sample sites because of less favorable magnetic recording properties in the more mauve-colored Edderfulgedal Formation and Tait Bjerg Member. Magnetozone thicknesses range from only a few meters (F3n.1r) to 86 m (F2r) and average around 23 m.

Correlation of Magnetostratigraphy to APTS. A critical age constraint in any viable attempt to correlate the magnetostratigraphic pattern to the APTS is the ETE, which has long been associated with the Kap Stewart Group (formerly Formation) on the basis of palynology and fossil megaflora (19, 21, 22). There is a marked facies change between the lacustrine gray mudstones and dolomitic marlstones and limestones of the Tait Bjerg Member of the Ørsted Dal Formation and the overlying black mudstones and coarse-grained and pebbly channel and sheet sandstones of the Kap Stewart Group, which has been interpreted to reflect an erosional unconformity at some localities (18, 20, 23). The abrupt megafloral turnover within the Kap Stewart Group also tends to be ascribed to a hiatus in sedimentation (21), although this view has been strongly disputed by others who maintain that strata containing the last occurrence of *Lepidopteris* designate the ETE in Greenland (19). We assume the ETE level is within the Kap Stewart Group whose base could

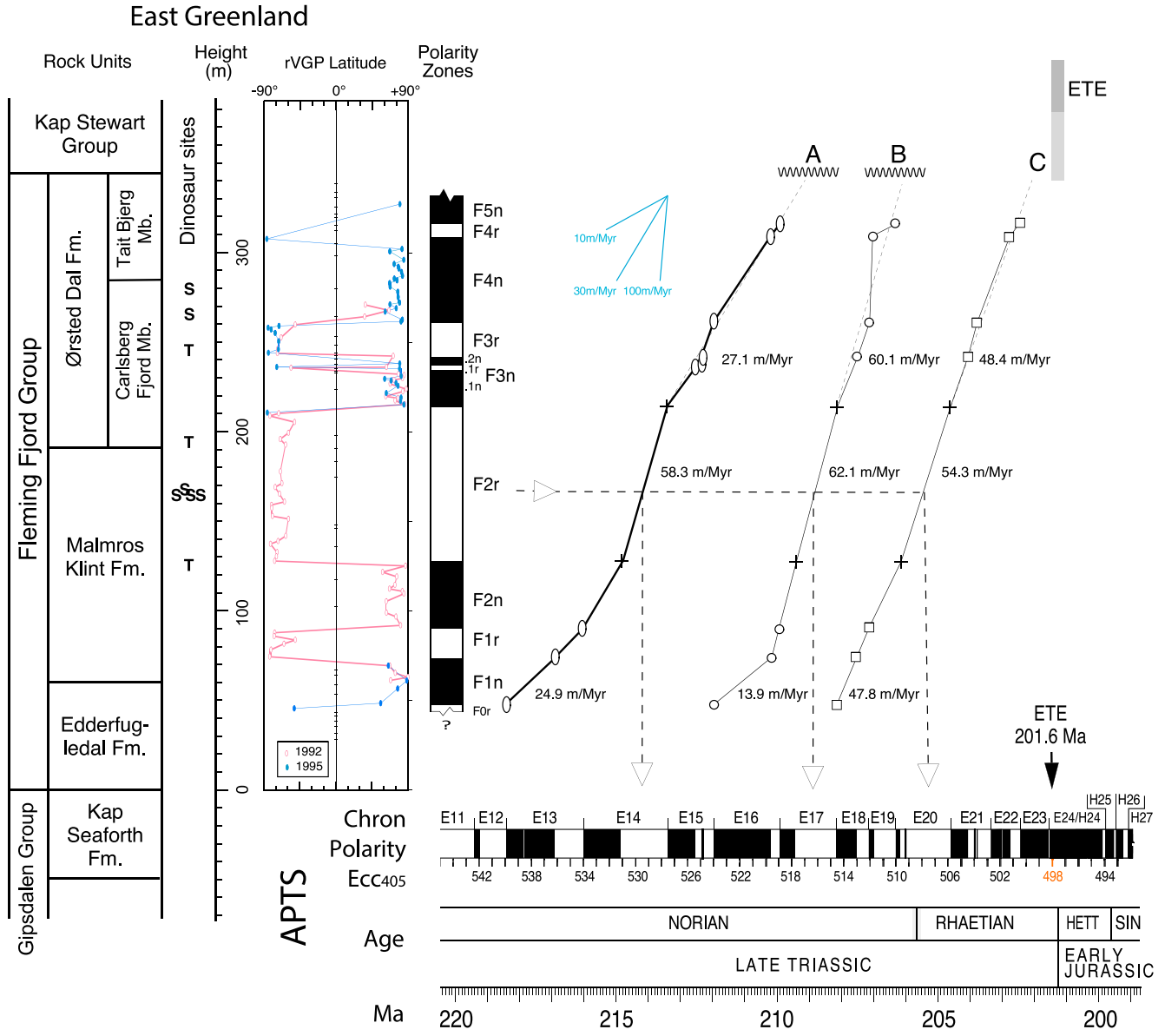

Fig. 3. The composite magnetostratigraphy for Fleming Fjord Group compared to the Newark-Hartford APTS (*SI Appendix*, Table S1). The rock units are according to ref. 18; stratigraphic occurrences of fossil dinosaurs are indicated by (*S*, sauropodomorph *Plateosaurus*) and (*T*, theropod) (14–16, 56–58). The rVGP latitude is the rotated latitude of the calculated virtual geomagnetic pole for the sample site C component direction compared to the mean overall paleomagnetic pole; the rVGP latitudes approaching +90° and −90° signify normal and reverse polarity, respectively. The ticks on the 0° axis are sampling levels that did not provide acceptable paleomagnetic data. The open and closed shading for polarity magnetozones are for reverse (suffix *r*) and normal (suffix *n*) polarity intervals that are labeled upward from F0r to F5n. The horizontal axis is APTS (12) showing polarity chrons, maxima in 405-ky eccentricity cycles (Ecc405) numbered from most recent maxima at 0.216 Ma and geologic ages in Ma. The correlation options labeled A, B, and C (*SI Appendix*, Table S2) are alternative links of the polarity magnetozone sequence to the APTS, all initially keyed to possible counterparts to long magnetozone F2r and within the younger age constraint of 201.6 Ma for the ETE recorded in the overlying Kap Stewart Group. The implied ages for earliest occurrence of the dinosaur *Plateosaurus* in upper Malmros Klint Formation for different correlation options are shown by dashed lines and open arrows. Option A is preferred (see text).

nevertheless be associated with an unconformity. The age of the ETE is well calibrated by U-Pb dating at 201.6 Ma (24) and was used to anchor the APTS (12).

The age of the underlying Fleming Fjord Group, especially the Malmros Klint and Ørsted Dal formations, has been loosely attributed to the late Norian-Rhaetian based on vertebrate fossil assemblages (18). For numerical reference, the Norian/Rhaetian boundary has been placed at 205.5 Ma based on U-Pb dating of a marine bivalve biostratigraphy in Peru (25) or at 209.5 Ma based on magnetostratigraphic correlation of a proposed boundary stratotype section with a conodont zonation in Austria to the APTS (26) via the Pizzo Mondello marine section in Sicily (27). There seems to be better agreement on the definition and age of the Carnian/Norian boundary, which is placed at about 227 Ma based on correlation of the ammonoid and conodont-bearing Pizzo Mondello section to the APTS (27). The available data thus suggests the Rhaetian is ∼4 or 8 My long [the so-called "short-" and "long-Rhaetian" options (28)], and the Norian is, in complement, 21.5 to 17.5 My long.

For purposes of correlation, the APTS for the Triassic is assumed to be complete. It was constructed from data of cores with virtually complete recovery of the kilometers-thick Newark basin

section with sediment accumulation rates of ~150 m/My and higher; moreover, significant portions of the polarity sequence have been successfully replicated in various sections regionally [e.g., Dan River Basin (29)] and farther afield, especially the Colorado Plateau where the temporal astronomical pacing assumed in the APTS has been verified by high-precision U-Pb dating (9, 10). The polarity interval lengths conform to a Poisson distribution and average around 0.5 My [~2 reversals per My; (30)]. The presence of 12 polarity magnetozones in the Fleming Fjord Group would thus imply an overall duration of roughly 6 My.

With these general constraints in mind, cross-plots of a range of correlation options (from older to younger: A, B, and C) between the Fleming Fjord Group composite magnetostratigraphy and the APTS are shown in Fig. 3 and listed in *SI Appendix*, Table S4. The three correlation options are keyed to thick magnetozone F2r, which at 86.35 m represents about one-quarter of the sampled 325-m thick composite magnetostratigraphy. In Option A, magnetozone F2r is correlated to 1.48-My-long Chron E14r, which would imply a sediment accumulation rate of 58.3 m/My for this interval. If the adjoining magnetozones are correlated to the APTS, magnetozones F1n-F1r-F2n stratigraphically below F2r correspond to chrons E13n-E13r-E14n, with only short Subchron E13n.1r apparently missing in F1n, and magnetozones F3n-F3r-F4n-F4r-F5n immediately above F2r correspond to chrons E15n-E15r-E16n-E16r-E17n with high fidelity, such that even short magnetozone F3n.1r has a plausible counterpart in Subchron E15r.1r. However, this fit requires long-term variations in sediment accumulation rates of about a factor of two: 24.9 m/My stratigraphically below, 58.3 m/My within, and 27.1 m/My above magnetozone F2r.

In Option B, which had been the favored original correlation (13), magnetozone F2r is correlated to 1.39-My-long Chron E17r, which would imply a sediment accumulation rate of 62.1 m/My for this interval, not that different from Option A. However, difficulties emerge with Option B in that relatively thin (25-m-thick) magnetozone F1n is correlated to a 1.8-My-long Chron E16n, implying a low sediment accumulation rate of only 13.9 m/My, whereas a 47.5-m-thick magnetozone F4n is correlated to only a 0.15-My-long Chron E19n, implying a contrastingly high sediment accumulation rate of 316.7 m/My that is more than a factor of 5 higher than for magnetozone F2r. Also bothersome with this correlation is that there is no obvious counterpart in the APTS to thin magnetozone F3n.1r.

In Option C, the youngest of the correlation options considered, magnetozone F2r is correlated to 1.59-My-long Chron E20r, which would imply a sediment accumulation rate of 54.3 m/My for this interval. A distinguishing feature of this correlation scheme is that it could be accommodated by much the same rate of sediment accumulation over the entire section: 47.8 m/My below, 54.3 m/My within, and 48.4 m/My above magnetozone F2r. On the other hand, normal polarity magnetozone F2n does not capture the multiple reversal sequence of chrons E19n-E19r-E20n if magnetozone F2r were to be equated to Chron E20r. The disjuncture is also in disagreement of dominant polarity in that normal polarity magnetozone F2n would need to be correlated to an interval of predominantly reverse polarity including the 0.69-My-long Subchron E19r.

The three correlation options would imply that the Fleming Fjord Group represents about 8 My (218 to 210 Ma, mid to late Norian) for Option A, 6 My (212 to 206 Ma, late Norian) for Option B, or 6 My (208 to 202 Ma, late Norian-Rhaetian) for Option C. None of the correlation options violate independent, albeit meager, age constraints. Major cycle thicknesses of 5 to 6 m in lithological variations in the Malmros Klint Formation and ascribed to the 100-ky Milankovich climate cycle would indicate sediment accumulation rates of ~54 m/My (31), consistent with any of the three options for magnetozone F2r that encompasses the middle to upper Malmros Klint and lower Ørsted Dal formations. However, Options A and B would imply an unconformity of a 4- to 8-My duration with respect to the overlying Kap Stewart Group should it contain the ETE, whereas Option C would allow depositional continuity between the Ørsted Dal Formation and the Kap Stewart Group.

However, the appeal of a fairly uniform sediment accumulation rate for the entire section with Option C comes at the expense of requiring a low fidelity polarity record in the lower part. This weakness in the magnetostratigraphic correlation makes us disinclined to accept Option C as providing a valid age model. In contrast, Option B has high magnetostratigraphic fidelity with essentially all polarity chrons accounted for but requires huge swings in sediment accumulation rate to correlate the magnetozones in the lower and upper parts of the section. Option B was initially preferred (13) but has become less tenable with the downward and upward extension of the original magnetostratigraphy. We therefore explore the implications of now-favored Option A, which has a good fidelity magnetostratigraphic record with long-term changes in sediment accumulation rate that are large but seem compatible with changes in lithology (e.g., higher rate in the most sand-rich facies in the Malmros Klint Formation).

For Option A, extrapolating the sediment accumulation rate of 27.1 m/My for magnetozones F3n to F5n stratigraphically upward gives an age of about 209 Ma for the top of the Ørsted Dal Formation; if the base of the Kap Stewart Group is no older than about 202 Ma (assuming the 201.6 Ma ETE is recorded within the unit), this would imply a depositional gap of some 8 My between the Ørsted Dal Formation and the Kap Stewart Group. The upward extrapolation to only 209 Ma also implies that the Fleming Fjord Group is of mostly Norian age, irrespective of the "short" or "long" Rhaetian time scale proposals. Extrapolating the sediment accumulation rate of 24.9 m/My for magnetozones F2n to F1n downward to the contact 47 m below with the underlying Kap Seaforth Formation of the Gipsdalen Group would add 1.89 My and give an age of ~220 Ma, or early Norian, for the base of the Fleming Fjord Group. This is somewhat younger but not grossly inconsistent with an age range of 226 to 235 Ma (Carnian-early Norian) assigned to the Gipsdalen Group on the basis of rather uncertain biostratigraphic constraints (32). Stratigraphically below the Gipsdalen Group, the continental Pingo Dal Group is also notably lacking in age-diagnostic fossils (32). Only the underlying Wordie Creek Group with a rich ammonoid fauna has had a firm age assignment for the Triassic of East Greenland [Induan, Early Triassic (33)]; its marine deposition was followed by syn-rift alluvial progradation and postrift continental deposition, which dominated the rest of the Triassic in the region (18, 34).

Distribution of Dinosaurs in the Late Triassic. The configuration of Pangea in the Triassic is well established from backtracking the constituent continents from sea floor spreading histories and fitting continent–ocean boundaries (35), whereas the paleolatitudinal framework is established from paleomagnetic data, in this case, using mean global pole positions for 230, 220, 210, and 200 Ma (Table 6 in ref. 36). We interpolate between the 220- and 210-Ma poles to estimate a paleolatitude of 43.3 ± 2.6°N at 215 Ma for Jameson Land of central East Greenland at 215 Ma. This compares favorably to a mean paleolatitude of 40.9°N determined from the Fleming Fjord Group sample data corrected for inclination flattening (8). Paleolatitudes similarly interpolated at 215 Ma for some other sites under discussion (Fig. 1) are 45°S for the Ischigualasto-Villa Union basin (Los Colorados Formation) in northwestern Argentina, 9°N for the Petrified Forest National Park (PFNP) of Arizona in the North American Southwest, and 36°N for the Germanic basin in continental Europe, all with 95% confidence uncertainties of 2.6° (Fig. 4).

The earliest well-dated dinosaur occurrences are in the Southern Hemisphere, notably in the Santa Maria Formation in the Parana basin of southern Brazil [e.g., basal sauropodomorph

Saturnalia (3)] dated to 233 Ma (5), and the Ischigualasto Formation of northwestern Argentina [e.g., early theropod *Herrerasaurus* (1, 37, 38)] dated to ∼230 Ma (4), which is overlain by the Los Colorados Formation, a ∼600-m-thick succession of continental deposits spanning 227 to 212.5 Ma according to magnetochronology (6) and containing a vertebrate assemblage in its upper part (La Esquina fauna, correlated to magnetozones LC7r and LC8n = chrons E14r and E15n of the APTS, 215 to 212.5 Ma) that is rich in dinosaurs (2) such as, sauropodomorph *Coloradisaurus* (39). Recently published U-Pb dates from the lower Elliot Formation in the Karoo basin of southern Africa support temporal correlations of some of its fauna, including the sauropodomorph *Plateosauravus*, to that of the Los Colorados Formation (40).

The best-documented, earliest dinosaur occurrences in North America come from the Chinle Formation. Theropods of arguable affinities ["*Camposaurus*"; (41)] have been reported from the *Placeria*s Quarry in Arizona (42, 43) where a U-Pb detrial zircon date of 219.39 ± 0.16 Ma was obtained on the main Bone Bed (44). However, recycled zircons are prevalent in the lower Chinle Formation (45) and may be responsible for apparent age disagreements of several million years; for example, a sample (SBJ) from an outcrop in the Sonsela Member with a high-precision U-Pb detrital zircon date of 219.32 ± 0.26 Ma (46) seems to correspond to age estimates that are 2 to 4 My younger for the Sonsela Member in the PFNP-1A drill core (10, 47). Such uncertainties directly affect the dating of the major biotic turnover at the Adamanian–Revueltian transition that is usually placed somewhere within the Sonsela Member (48). Magnetostratigraphic correlations show that the Sonsela Member in the PFNP-1A core encompasses chrons E14n–E15n, spanning 216 to 213 Ma (10), but which would extend back to as much as 220 Ma if U-Pb detrital zircon dates in the lower Chinle Formation (44, 47) were to be taken at face value. In any case, a more securely constrained dinosaur fauna of the Chinle Formation is found at Hayden Quarry at Ghost Ranch in New Mexico, where taxa including the early theropod *Tawa* and *Chindesaurus,* a possible rare example of a herrerasaurid theropod dinosaur from outside South America [(49); but see (50)] have been described. A U-Pb zircon date in Hayden Quarry of 211.9 ± 0.7 Ma (51) is consistent with the occurrence of a similar fossil assemblage in the Petrified Forest Member of the Chinle Formation in PFNP in Arizona (52), where its age is well constrained between ∼209 and 212.5 Ma by congruent U-Pb zircon geochronology and magnetochronology (9, 46).

At higher latitudes in the Northern Hemisphere, the earliest well-dated occurrence of dinosaurs in Europe, in this case the plateosaurid *Plateosaurus*, is in the Löwenstein Formation of the Keuper Group in the Germanic basin (53, 54). This formation also contains the conchostracan *Shipingia*, whose first appearance is in the oldest part of the Passaic Formation of the Newark sequence (17), which corresponds to Chron E13n with an estimated age of around 217 Ma in the APTS (12). *Shipingia* is also associated with the Alaunian substage which, on the basis of conodont biostratigraphy and magnetostratigraphy at Silicka Brezova (Slovakia), extends up through Chron E15n (55) and hence provides an age range of ∼217 to 212.5 Ma according to the APTS for the dinosaur-bearing Löwenstein Formation.

At the northernmost known paleolatitude fossil sites, in East Greenland, *Plateosaurus* bone fossils have been found in a half-dozen sites from at least four different stratigraphic levels in the Malmros Klint Formation (from as low as 25 m below its contact with the Ørsted Dal Formation) and the Carlsberg Fjord Member, where a complete skeleton was found at Lepidopteriselv (Fig. 2) 5 m below its contact with the Tait Bjerg Member (14–16). There are also preliminary reports of theropod bone fossils in the middle ("Theropod Mound") and lowermost Carlsberg Fjord Member (56, 57) and in the middle of the Malmros Klint Formation as far down as 65 m below its top (58). The earliest documented occurrence of *Plateosaurus* is in the middle part of magnetozone F2r, which, according to the age model of Option A, is within Chron E14r and corresponds to an interpolated age of 214.2 Ma (Fig. 4). The oldest reported theropod site would be near the base of magnetozone F2r, corresponding to a somewhat older age of about 214.8 Ma. These datum levels for oldest dinosaur fossils are about 5 My older than estimated from our superceded age model (Option B, Fig. 3) and would place them in a very different phase of suggested effects of 10-My–scale monsoon dynamics in the Late Triassic (59).

Discussion

From the foregoing, a review of global chronostratigraphic evidence suggests that, after appearing by around 230 Ma in the temperate belt of Gondwana in the Southern Hemisphere (as recorded by fossils in well-dated units like the Ischigualasto Formation of northwestern Argentina and the Santa Maria Formation in southern Brazil), bone fossils of sauropodomorph dinosaurs are not found in strata of the Northern Hemisphere until 217 to 212.5 Ma in the Germanic Basin of Europe (Löwenstein Formation) and more precisely at close to 214 Ma in Jameson Land of central East Greenland (Malmros Klint Formation). The great circle distance across Pangea between Jameson Land and northwestern Argentina was vast, about 95° of arc or over 10,000 km but with no intervening major seaways or high mountain ranges, a route should have been traversable by land-bound terrestrial vertebrates (Fig. 1). Yet, something evidently held sauropodomorphs back for about 15 My from dispersing widely until around 214 Ma when they show up in the temperate belt (northern Europe, Greenland) of the Northern Hemisphere. Interestingly, there is scant evidence of sauropodomorphs in the entire Triassic of North America (e.g., Chinle and Newark Supergroup) and northern Africa (Argana basin, Morocco), which evidently were not areas to linger being within or close to the tropical arid belt.

Given a tectonically stable supercontinent assembly of Pangea, barriers to dispersal were most likely climatological. The Late Triassic was a time of generally very high atmospheric pCO_2 values according to empirical estimates from pedogenic carbonate barometry (60) that are broadly consistent with carbon cycle models (61) (Fig. 4). Climate modeling studies show that higher atmospheric pCO_2 values are associated with more accentuated contrasts between climate belts, especially in precipitation to evaporation (P-E) (62). The more arid climate belts that ecologically separated the southern temperate belt of Gondwana, where dinosaurs apparently originated, from eventual venues in the hospitable counterpart northern temperate belt of Laurasia (Europe and Greenland) may have presented formidable barriers to dispersal. Moreover, the low latitudes of North America in the interior of Pangea in a high-pCO_2 world would have experienced extreme climate fluctuations that affected plant communities and help to explain the rarity to virtual absence of herbivorous sauropodomorphs (63) and related vertebrates (64) in this near-equatorial setting.

After more or less steadily high pCO_2 values of around 4,000 parts per million (ppm) for the initial half of the Late Triassic (∼233 to 215 Ma), the pedogenic carbonate pCO_2 data show that atmospheric pCO_2 values plunged to around 2,000 ppm at 215 to 212 Ma before increasing again to high values (60) (Fig. 4). This interval of reduced pCO_2 levels has been documented in contemporaneous paleosols from widely separated sites in the Newark, Hartford, and Chama basins (60), including Hayden Quarry at Ghost Ranch in New Mexico with the theropods *Tawa* and *Chindesaurus* (63). By synchronizing $\delta^{18}O$ records of sea-surface temperature change to the Newark pedogenic pCO_2 record embedded within the APTS, Knobbe and Schaller (65) demonstrate that the response for a halving of pCO_2 is in good

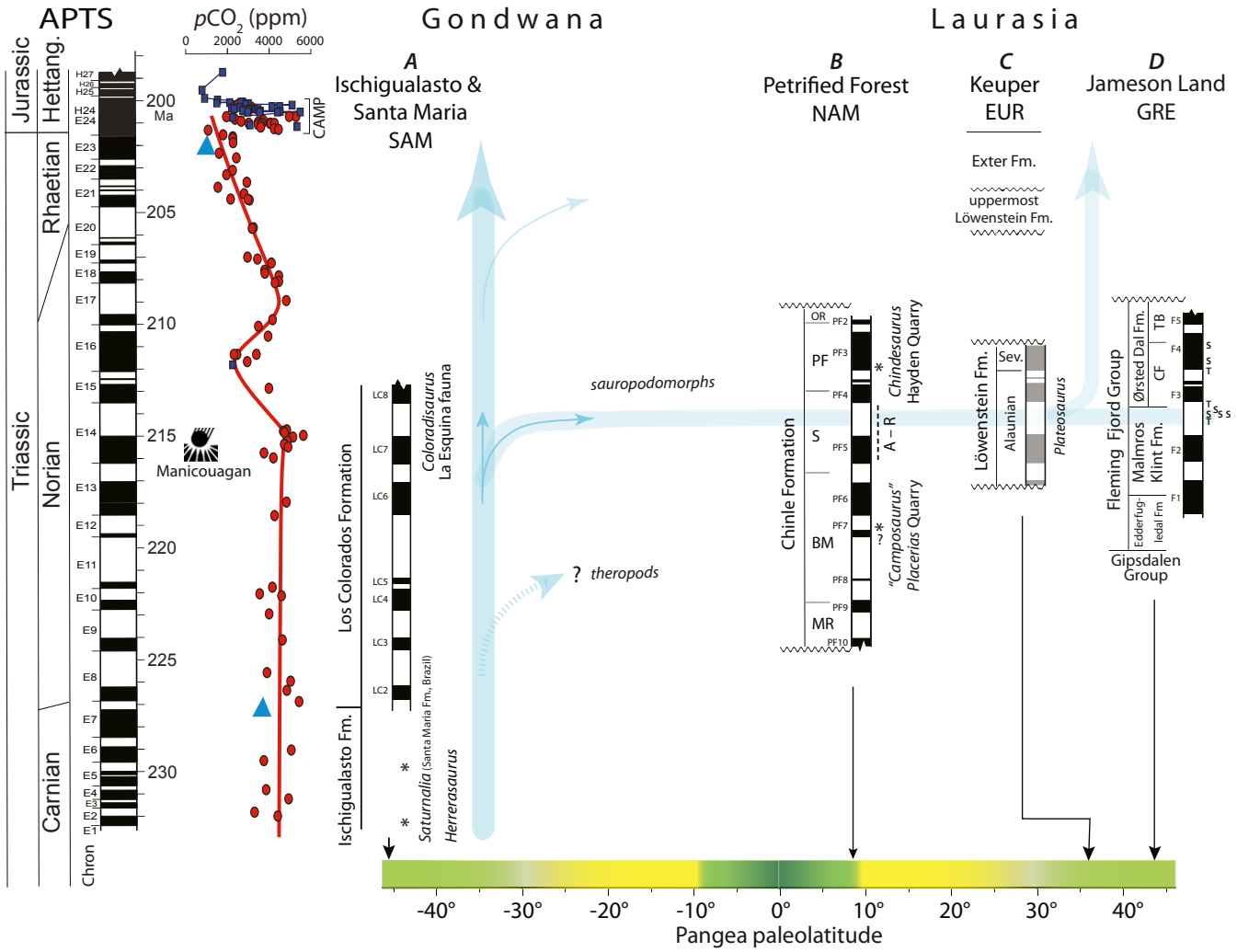

Fig. 4. Independently dated Late Triassic dinosaur-bearing sedimentary sections across the Pangea supercontinent keyed to the Newark-Hartford APTS (12) for the Late Triassic (Carnian–Norian–Rhaetian) to Early Jurassic (Hettangian) where normal/reverse polarity chrons (filled/open bars) are labeled E1 to E24 (Newark basin) and H24 to H27 (Hartford basin). The atmospheric pCO_2 values from pedogenic carbonates (60) in the Newark basin (red circles; systematic error bars typically ±2,000 ppm are omitted for clarity), one determination in the Hartford basin (small pink square), and from sediments interbedded with lavas of the Central Atlantic magmatic province (CAMP; blue squares), with model outputs of GEOCLIM (61) shown by two blue triangles. Column A: Ischigualasto-Villa Union and associated basins in northwestern Argentina with U-Pb zircon date of 229 Ma (4) from the lower Ischigualasto Formation with early dinosaurs like the theropod *Herrerasaurus* [and the basal sauropodomorph *Saturnalia* from the age-correlative Santa Maria Formation of southern Brazil dated to 233 Ma (5)] and magnetostratigraphy of the Los Colorados Formation (6) with La Esquina fauna, including *Coloradisaurus* (2), in the uppermost part. Paleolatitude of 46°S at 215 Ma (see text). Column B: Magnetostratigraphy of Chinle Formation in core PFNP-1A from Petrified Forest National Park in Arizona (10) with U-Pb zircon dates validating APTS back to about 215 Ma (9). Chinle members shown are labeled as follows: OR, Owl Rock; PF, Petrified Forest; S, Sonsela; BM, Blue Mesa; and MR, Mesa Redondo. The age of *Chindesaurus* from Hayden Quarry is constrained by U-Pb zircon date of 211.9 ± 0.7 Ma (51). The Adamanian–Revueltian land vertebrate transition (A–R) is loosely associated with middle part of Sonsela Member (52). A coelophysoid theropod ("*Camposaurus*") reported from the *Placerias* Quarry in Arizona (42, 43) is associated with a U-Pb zircon date of 219.39 ± 0.16 Ma (44) that would make it one of the oldest dinosaur occurrences in the Northern Hemisphere although there are issues with recycled zircons in the lower Chinle Formation (45, 47). Paleolatitude of 7°N at 215 Ma. Column C: The *Plateosaurus*-bearing Löwenstein Formation in the Keuper Group of Germanic basin (17) whose age assignment is based on biostratigraphic correlations for Alaunian to marine magnetostratigraphic sections (27, 55). Paleolatitude of 37°N at 215 Ma. Column D: The composite magnetostratigraphic section for Fleming Fjord Group of East Greenland using correlation Option A (this study). Stratigraphic levels with sauropodomorph (*Plateosaurus*) fossil sites are indicated by "S" and theropod fossil sites by "T" (see Fig. 3). Paleolatitude of 43°N at 215 Ma. The color bar on the paleolatitude scale along the bottom shows the relative precipitation minus evaporation (P – E) values as a function of latitude, with a green shade indicating more positive values (wet) and a yellow shade indicating more negative values (arid), based on a generalized general circulation model of the coupled ocean-atmosphere climate system (62). The Manicouagan impact event is shown at tentative date of 215.5 Ma (70).

agreement with other results showing that atmospheric pCO_2 was a dominant control on Earth's climate in an ice-free world of the Triassic. This lends support to generalized coupled ocean-atmosphere climate models (62) showing that a large reduction of pCO_2 would reduce P-E contrast between the tropical desert belt(s) and the equatorial humid belt, as well as reduce the severity of Milankovich-induced climate fluctuations such as monsoons in low latitudes (66, 67). The lowered climate contrasts are what may have provided opportunities for dinosaurs and associated terrestrial vertebrate fauna (64) to traverse climate zones and significantly expand their geographic range at around 214 Ma. Carnivorous theropods may not have been as subject to the same climatological constraints given their presence in North America (50), which some reports suggest may

have arrived earlier there (68) as well as in East Greenland (57, 58).

The cause of the mid-Norian dip in atmospheric pCO_2 is unclear. Long term monsoonal effects may have played a role, although the suggested timing of the mid-Norian dinosaur dispersal is now a few million years earlier than the ∼212 Ma that had been considered (59). According to correlation networks, the dip in pCO_2 seems to shortly follow a large excursion in $\delta^{13}C$ recorded in marine carbonates at Pizzo Mondello centered on Chron E14n [∼216 to 215 Ma (69)], again pointing to a major perturbation in the global carbon cycle in the Alaunian interval that might be coupled to the dip in pCO_2. The 85-km-diameter Manicouagan impact crater in Canada with a preliminary U-Pb zircon date of 215.5 Ma (70) and that had far-field effects (71) provides a possible trigger of cascading events eventually affecting climate, for example, widespread deforestation, erosion, and increased weathering consumption of pCO_2. The intriguing near-coincidence in timing among the Manicouagan impact, $\delta^{13}C$ excursion, and dip in atmospheric pCO_2 with our postulated mid-Norian dinosaur dispersal event (and perhaps the Adamanian–Revueltian biotic turnover) requires more precise age registry to determine how these phenomena might be arrayed in a plausible temporal sequence to explore possible modes of causality.

Conclusions

An updated age model for the fossiliferous Fleming Fjord Group of central East Greenland places the first occurrences of sauropodomorph dinosaurs at their northernmost range in Laurasia at about 214 Ma, long after their initial appearance at about 230 Ma at their southernmost range in Gondwana. The Late Triassic tended to have very high atmospheric pCO_2 values, which climate models suggest would result in intensified aridity in the desert belts and extreme swings in humidity and aridity at equatorial latitudes. These prevailing conditions are suggested to have acted as barriers for dispersal that kept herbivorous sauropodomorph dinosaurs corralled in the southern temperate belt of Pangea. Their apparent breakout by ∼214 Ma occurs within a large reported drop in atmospheric pCO_2 concentration at 215 to 212 Ma, which may have lowered climate barriers and allowed rapid dispersal of sauropodomorphs to the far reaches of Europe and Greenland in the Northern Hemisphere temperate belt. Direct evidence is still lacking of sauropodomorphs in their presumed passage across the low paleolatitudes of North America where theropod dinosaurs are, however, present as a rare component of some Triassic vertebrate assemblages and may even be older than 214 Ma, representing more sporadic dispersals not obviously related to climate thresholds. On the other hand, decreasing atmospheric pCO_2 values over the last ∼8 million years of the Triassic, essentially the Rhaetian, might have resulted in further climate-induced dispersal opportunities for the sauropodomorphs.

Materials and Methods

The same paleomagnetic sampling and analytical procedures described for the 1992 field season at Tait Bjerg (13) were followed for the 1995 sampling campaign at "Track Mountain" (MacKnight Bjerg) as described in the *SI Appendix*. Site-level data sets (*SI Appendix*, Tables S1 and S2) were used for the composite magnetostratigraphy of the Fleming Fjord Group shown in Fig. 3.

Data Availability. All study data are included in the article and/or *SI Appendix*.

ACKNOWLEDGMENTS. We thank our host institutions for patient and generous support of this research, including the Paleomagnetic Research Fund at Lamont-Doherty and for various NSF grants, most recently EAR-0958859 (D.V.K.), to the Carlsberg Foundation (L.B.C.) for logistical support in Greenland, and the late Farish A. Jenkins of the Museum of Comparative Zoology at Harvard University for organizing and providing support for the 1992 and 1995 field seasons and inviting D.V.K. to join. We are grateful to colleagues Paul Olsen, Giovanni Muttoni, and Morgan Schaller for productive, ongoing discussions on wide-ranging Triassic matters and Malte Mau, Octávio Mateus, and Jesper Milàn on the Greenland record, in particular. We greatly appreciate the thoughtful and constructive comments by the journal reviewers, which allowed us to improve the manuscript. This is Lamont-Doherty Earth Observatory Contribution 8469.

1. R. R. Rogers *et al*., The Ischigualasto tetrapod assemblage (Late Triassic, Argentina) and 40Ar/39Ar dating of dinosaur origins. *Science* **260**, 794–797 (1993).
2. R. N. Martínez *et al*., A basal dinosaur from the dawn of the dinosaur era in southwestern Pangaea. *Science* **331**, 206–210 (2011).
3. M. C. Langer, M. D. Ezcurra, J. S. Bittencourt, F. E. Novas, The origin and early evolution of dinosaurs. *Biol. Rev. Camb. Philos. Soc.* **85**, 55–110 (2010).
4. J. B. Desojo *et al*., The late Triassic Ischigualasto Formation at Cerro Las Lajas (La Rioja, Argentina): Fossil tetrapods, high-resolution chronostratigraphy, and faunal correlations. *Sci. Rep.* **10**, 12782 (2020).
5. M. C. Langer, J. Ramezani, Á. A. S. Da Rosa, U-Pb age constraints on dinosaur rise from south Brazil. *Gondwana Res.* **57**, 133–140 (2018).
6. D. V. Kent, P. Santi Malnis, C. E. Colombi, O. A. Alcober, R. N. Martínez, Age constraints on the dispersal of dinosaurs in the late Triassic from magnetochronology of the Los Colorados Formation (Argentina). *Proc. Natl. Acad. Sci. U.S.A.* **111**, 7958–7963 (2014).
7. S. L. Brusatte *et al*., The origin and early radiation of dinosaurs. *Earth Sci. Rev.* **101**, 68–100 (2010).
8. D. V. Kent, L. Tauxe, Corrected late Triassic latitudes for continents adjacent to the North Atlantic. *Science* **307**, 240–244 (2005).
9. D. V. Kent *et al*., Empirical evidence for stability of the 405-kiloyear Jupiter-Venus eccentricity cycle over hundreds of millions of years. *Proc. Natl. Acad. Sci. U.S.A.* **115**, 6153–6158 (2018).
10. D. V. Kent *et al*., Magnetochronology of the entire Chinle Formation (Norian age) in a scientific drill core from petrified forest National Park (Arizona, USA) and implications for regional and global correlations in the late Triassic. *Geochem. Geophys. Geosyst.* **20**, 4654–4664 (2019).
11. P. E. Olsen *et al*., Colorado plateau coring project, phase I (CPCP-I): A continuously cored, globally exportable chronology of Triassic continental environmental change from Western North America. *Sci. Drill.* **24**, 15–40 (2018).
12. D. V. Kent, P. E. Olsen, G. Muttoni, Astrochronostratigraphic polarity time scale (APTS) for the Late Triassic and Early Jurassic from continental sediments and correlation with standard marine stages. *Earth Sci. Rev.* **166**, 153–180 (2017).
13. D. V. Kent, L. B. Clemmensen, Paleomagnetism and cycle stratigraphy of the Triassic Fleming Fjord and Gipsdalen formations of East Greenland. *Bull. Geol. Soc. Den.* **42**, 121–136 (1996).
14. F. A. Jenkins *et al*., Late Triassic continental vertebrates and depositional environments of the Fleming Fjord formation, Jameson land, East Greenland. *Medd. Gronl. Geosci.* **32**, 1–25 (1994).
15. L. B. Clemmensen *et al*., The vertebrate-bearing late Triassic Fleming Fjord Formation of central East Greenland revisited: Stratigraphy, palaeoclimate and new palaeontological data. *Geol. Soc. Lond. Spec. Publ.* **434**, 31–47 (2016).
16. M. Marzola, O. Mateus, J. Milàn, L. Clemmensen, A review of Palaeozoic and Mesozoic tetrapods from Greenland. *Bull. Geol. Soc. Den.* **66**, 21–46 (2018).
17. G. H. Bachmann, H. W. Kozur, The Germanic Triassic: Correlations with the international chronostratigraphic scale, numerical ages and Milankovitch cyclicity. *Hallesches Jahrb. Geowiss. B* **26**, 17–62 (2004).
18. L. B. Clemmensen, D. V. Kent, M. Mau, O. Mateus, J. Milàn, Triassic lithostratigraphy of the Jameson land basin (central East Greenland), with emphasis on the new Fleming Fjord group. *Bull. Geol. Soc. Den.* **68**, 95–132 (2020).
19. J. C. McElwain, D. J. Beerling, F. I. Woodward, Fossil plants and global warming at the Triassic-Jurassic boundary. *Science* **285**, 1386–1390 (1999).
20. G. Dam, F. Surlyk, Cyclic sedimentation in a large wave- and storm-dominated anoxic lake; Kap Stewart formation (Rhaetian-Sinemurian), Jameson land, East Greenland. *Spec. Pubis Int. Sediment.* **18**, 419–448 (1993).
21. T. M. Harris, *The Fossil Flora of Scoresby Sound, East Greenland: Part 5: Stratigraphic Relations of the Plant Beds* (Meddelelser om Gronland, Kobenhavn, 1937), vol. 112, pp. 1–114.
22. K. R. Pedersen, J. J. Lund, Palynology of the plant-bearing rhaetian to Hettangian Kap Stewart formation, scoresby sund, East Greenland. *Rev. Palaeobot. Palynol.* **31**, 1–69 (1980).
23. G. Dam, F. Surlyk, Forced regressions in a large wave- and storm dominated anoxic lake, Rhaetian-Sinemurian Kap Stewart Formation, East Greenland. *Geology* **20**, 749–752 (1992).
24. T. J. Blackburn *et al*., Zircon U-Pb geochronology links the end-Triassic extinction with the central Atlantic magmatic province. *Science* **340**, 941–945 (2013).
25. J.-F. Wotzlaw *et al*., Towards accurate numerical calibration of the Late Triassic: High-precision U-Pb geochronology constraints on the duration of the Rhaetian. *Geology* **42**, 571–574 (2014).
26. S. K. Hüsing, M. H. L. Deenen, J. G. Koopmans, W. Krijgsman, Magnetostratigraphic dating of the proposed rhaetian GSSP at steinbergkogel (upper Triassic, Austria): Implications for the late Triassic time scale. *Earth Planet. Sci. Lett.* **302**, 203–216 (2011).
27. G. Muttoni *et al*., Tethyan magnetostratigraphy from Pizzo Mondello (sicily) and correlation to the late Triassic Newark astrochronological polarity time scale. *Geol. Soc. Am. Bull.* **116**, 1043–1058 (2004).
28. J. G. Ogg, C. Huang, L. Hinnov, Triassic timescale status: A brief overview. *Albertiana* **41**, 3–30 (2014).

29. P. E. Olsen, J. C. Reid, K. Taylor, J. H. Whiteside, D. V. Kent, Revised stratigraphy of Late Triassic age strata of the Dan River Basin (Virginia and North Carolina, USA) based on drill core and outcrop data. *Southeast. Geol.* **51**, 1–31 (2015).
30. D. V. Kent, P. E. Olsen, Astronomically tuned geomagnetic polarity time scale for the Late Triassic. *J. Geophys. Res.* **104**, 12831–12841 (1999).
31. L. B. Clemmensen, D. V. Kent, F. A. Jenkins Jr, A late Triassic lake system in East Greenland: Facies, depositional cycles and palaeoclimate. *Palaeogeogr. Palaeoclimatol. Palaeoecol.* **140**, 135–159 (1998).
32. S. D. Andrews, S. R. A. Kelly, W. Braham, M. Kaye, Climatic and eustatic controls on the development of a late Triassic source rock in the Jameson land basin, East Greenland. *J. Geol. Soc. London* **171**, 609 (2014).
33. F. Surlyk, M. Bjerager, S. Piasecki, L. Stemmerik, Stratigraphy of the marine lower Triassic succession at Kap Stosch, Hold with Hope, North-East Greenland. *Bull. Geol. Soc. Den.* **65**, 87–123 (2017).
34. P. Guarnieri, A. Brethes, T. M. Rasmussen, Geometry and kinematics of the Triassic rift basin in Jameson land (east Greenland). *Tectonics* **36**, 602–614 (2017).
35. A. L. Lottes, D. B. Rowley, "Reconstruction of the Laurasian and Gondwanan segments of Permian Pangaea" in *Palaeozoic Palaeogeography and Biogeography, Memoir 12*, W. S. McKerrow, C. R. Scotese, Eds. (Geological Society, London, 1990), pp. 383–395.
36. D. V. Kent, E. Irving, Influence of inclination error in sedimentary rocks on the Triassic and Jurassic apparent polar wander path for North America and implications for Cordilleran tectonics. *J. Geophys. Res.* **115**, B10103 (2010).
37. P. C. Sereno, C. A. Forster, R. R. Rogers, A. M. Monetta, Primitive dinosaur skeleton from Argentina and the early evolution of Dinosauria. *Nature* **361**, 64–66 (1993).
38. H.-D. Sues, S. J. Nesbitt, D. S. Berman, A. C. Henrici, A late-surviving basal theropod dinosaur from the latest Triassic of North America. *Proc. Biol. Sci.* **278**, 3459–3464 (2011).
39. C. Apaldetti, R. N. Martinez, D. Pol, T. Souter, Redescription of the skull of Coloradisaurus brevis (Dinosauria, sauropodomorpha) from the late Triassic Los Colorados Formation of the Ischigualasto-Villa Union basin, northwestern Argentina. *J. Vertebr. Paleontol.* **34**, 1113–1132 (2014).
40. E. Bordy *et al*., A chronostratigraphic framework for the upper Stormberg Group: Implications for the Triassic-Jurassic boundary in southern Africa. *Earth Sci. Rev.* **203**, 103120 (2020).
41. M. D. Ezcurra, S. L. Brusatte, Taxonomic and phylogenetic reassessment of the early neotheropod dinosaur Camposaurus arizonensis from the Late Triassic of North America. *Palaeontology* **54**, 763–772 (2011).
42. S. J. Nesbitt, R. B. Irmis, W. G. Parker, A critical reevaluation of the Late Triassic dinosaur taxa of North America. *J. Syst. Palaeontology* **5**, 209–243 (2007).
43. A. P. Hunt, S. G. Lucas, A. B. Heckert, R. M. Sullivan, M. G. Lockley, Late Triassic dinosaurs from the Western United States. *Geobios* **31**, 511–531 (1998).
44. J. Ramezani, D. E. Fastovsky, S. A. Bowring, Revised chronostratigraphy of the lower Chinle formation strata in Arizona and New Mexico (USA): High-precision u-pb geochronological constraints on the Late Triassic evolution of dinosaurs. *Am. J. Sci.* **314**, 981–1008 (2014).
45. G. E. Gehrels *et al*., LA-ICPMS U-Pb geochronology of detrital zircon grains from the Coconino, Moenkopi, and Chinle formations in the petrified forest National Park (Arizona). *Geochronology* **2**, 257–282 (2020).
46. J. Ramezani *et al*., High-precision U-Pb zircon geochronology of the late Triassic Chinle Formation, petrified forest National Park (Arizona, USA): Temporal constraints on the early evolution of dinosaurs. *Geol. Soc. Am. Bull.* **123**, 2142–2159 (2011).
47. C. Rasmussen *et al*., U-Pb zircon geochronology and depositional age models for the upper Triassic Chinle Formation (petrified forest National Park, Arizona, USA): Implications for late Triassic paleoecological and paleoenvironmental change. *Geol. Soc. Am. Bull.* **132**, 1–20 (2020).
48. J. W. Martz, W. G. Parker, Revised lithostratigraphy of the Sonsela member (Chinle Formation, upper Triassic) in the southern part of petrified forest National Park, Arizona. *PLoS One* **5**, e9329 (2010).
49. S. J. Nesbitt *et al*., A complete skeleton of a Late Triassic saurischian and the early evolution of dinosaurs. *Science* **326**, 1530–1533 (2009).
50. A. D. Marsh, W. G. Parker, New dinosauromorph specimens from Petrified Forest National Park and a global biostratigraphic review of Triassic dinosauromorph body fossils. *PaleoBios* **37**, 1–56 (2020).
51. R. B. Irmis, R. Mundil, J. W. Martz, W. G. Parker, High-resolution U–Pb ages from the Upper Triassic Chinle Formation (New Mexico, USA) support a diachronous rise of dinosaurs. *Earth Planet. Sci. Lett.* **309**, 258–267 (2011).
52. W. G. Parker, J. W. Martz, The Late Triassic (Norian) Adamanian–Revueltian tetrapod faunal transition in the Chinle Formation of petrified forest National Park, Arizona. *Earth Environ. Sci. Trans. R. Soc. Edinb.* **101**, 231–260 (2011).
53. A. M. Yates, The species taxonomy of the sauropodomorph dinosaurs from the Löwenstein Formation (Norian, Late Triassic) of Germany. *Palaeontology* **46**, 317–337 (2003).
54. D. B. Weishampel *et al*., "Dinosaur distribution" in *The Dinosauria*, D. B. Weishampel, P. Dodson, H. Osmólska, Eds. (University of California Press, 2004).
55. J. E. T. Channell *et al*., Carnian-Norian biomagnetostratigraphy at Silicka Brezova (Slovakia): Correlation to other Tethyan sections and to the Newark basin. *Palaeogeogr. Palaeoclimatol. Palaeoecol.* **191**, 65–109 (2003).
56. T. Sulej, A. Wolniewicz, B. Blazejowski, G. Niedźwiedzki, M. Tałanda, New perspectives on the late Triassic vertebrates of East Greenland: Preliminary results of a polish-Danish palaeontological expedition. *Pol. Polar Res.* **35**, 541–552 (2014).
57. G. Niedźwiedzki, T. Sulej, "Theropod dinosaur fossils from the Gipsdalen and Fleming Fjord formations (Carnian-Norian, Upper Triassic), East Greenland" in *34th Nordic Geological Winter Meeting*, H. A. Nakrem, A. M. Husås, Eds. (Geological Society of Norway, Oslo, Norway, 2020), p. 151.
58. M. Marzola, "The Late Triassic vertebrate fauna of the Jameson Land Basin, East Greenland: description, phylogeny, and paleoenvironmental implications," PhD thesis, Universida Nova de Lisboa, Lisbon, Portugal (2019).
59. M. Ikeda, K. Ozaki, J. Legrand, Impact of 10-Myr scale monsoon dynamics on Mesozoic climate and ecosystems. *Sci. Rep.* **10**, 11984 (2020).
60. M. F. Schaller, J. D. Wright, D. V. Kent, A 30 million-year record of Late Triassic pCO2 variation supports a fundamental control of the carbon-cycle by changes in continental weathering. *Geol. Soc. Am. Bull.* **127**, 661–671 (2015).
61. Y. Goddéris *et al*., Causal or casual link between the rise of nannoplankton calcification and a tectonically-driven massive decrease in Late Triassic atmospheric CO2? *Earth Planet. Sci. Lett.* **267**, 247–255 (2008).
62. S. Manabe, K. Bryan, CO2-induced change in a coupled ocean-atmosphere model and its paleoclimatic implications. *J. Geophys. Res.* **90**, 11689–11707 (1985).
63. J. H. Whiteside *et al*., Extreme ecosystem instability suppressed tropical dinosaur dominance for 30 million years. *Proc. Natl. Acad. Sci. U.S.A.* **112**, 7909–7913 (2015).
64. J. H. Whiteside, D. S. Grogan, P. E. Olsen, D. V. Kent, Climatically driven biogeographic provinces of Late Triassic tropical Pangea. *Proc. Natl. Acad. Sci. U.S.A.* **108**, 8972–8977 (2011).
65. T. K. Knobbe, M. F. Schaller, A tight coupling between atmospheric pCO2 and sea-surface temperature in the Late Triassic. *Geology* **46**, 43–46 (2017).
66. T. Yonetani, H. B. Gordon, Simulated changes in the frequency of extremes and regional features of seasonal/annual temperature and precipitation when atmospheric CO2 is doubled. *J. Clim.* **14**, 1765–1779 (2001).
67. A. Seth *et al*., Monsoon responses to climate changes—Connecting past, present and Future. *Curr. Clim. Change Rep.* **5**, 63–79 (2019).
68. A. J. Fitch, D. M. Lovelace, M. R. Stocker, "The oldest dinosaur from the Northern Hemisphere and the origins of Theropoda" in *Society of Vertebrate Paleontology 80th Annual Meeting* (Society of Vertebrate Paleontology, 2020).
69. G. Muttoni *et al*., A middle–late Triassic (Ladinian–Rhaetian) carbon and oxygen isotope record from the Tethyan ocean. *Palaeogeogr. Palaeoclimatol. Palaeoecol.* **399**, 246–259 (2014).
70. M. C. van Soest *et al*., (U-Th)/He dating of terrestrial impact structures: The Manicouagan example. *Geochem. Geophys. Geosyst.* **12**, Q0AA16 (2011).
71. H. Sato, T. Onoue, T. Nozaki, K. Suzuki, Osmium isotope evidence for a large Late Triassic impact event. *Nat. Commun.* **4**, 2455 (2013).